

Measurement of Berry's Phase for Noncyclic Evolution

Harald Weinfurter

Hahn-Meitner-Institut, Glienickerstrasse 100, D-1000 Berlin 39, Germany

Gerald Badurek

Institut für Kernphysik, Technical University Vienna, Schüttelstrasse 115, A-1020 Wien, Austria

(Received 27 November 1989)

Tracing the neutron spin on its passage through a magnetic field which rotates at various frequencies, it was possible to observe geometrically induced phase shifts of a quantum-mechanical state even for incomplete revolutions of this field. The experiments show that we can extract such purely geometric effects also from nonadiabatic evolutions.

PACS numbers: 03.65.Bz, 28.20.-v, 29.75.+x

The geometric effect on the phase of the wave function of an adiabatically changing quantum-mechanical system was first described by Berry¹ for cyclic evolutions of the Hamiltonian. Some more general approaches extended the applicability of this concept to homological problems and gauge theories² and described the connection to its classical analog, the Hannay angle.³ The first experimental manifestation of this geometric phase was found a few years after its theoretical formulation by observing the rotation of linearly polarized light on transmission through a twisted optical fiber.⁴ A similar experiment with particle beams was realized by tracing the neutron spin in adiabatically rotating magnetic fields.⁵ In the meantime, geometric phase shifts were also found by several other techniques such as, e.g., nuclear magnetic resonance,⁶ laser interferometry,⁷ and electron diffraction.⁸ The topological effect could also be deduced by dropping the condition for an adiabatic change of the system's parameter.⁹ Recently several authors pointed out theoretically that besides the dynamical phase shift there should also be an observable geometric effect for partial cycles and for open, noncyclic evolutions in parameter space.¹⁰⁻¹²

In the present Letter the interaction of neutrons with time-dependent rotating magnetic fields was used to prove these new ideas experimentally. The behavior of neutrons in magnetic fields is described by the Pauli equation with the Hamiltonian $H(t) = -\mu\sigma \cdot \mathbf{B}(t)$,

where μ is the magnetic moment of the neutron and σ is the Pauli spinor operator. It is well known that for the case of a field $\mathbf{B}(t) = B[\hat{x}\cos(\omega t) + \hat{y}\sin(\omega t)]$ rotating in the \hat{x} - \hat{y} plane with constant frequency ω and field strength B an analytical solution of the Pauli equation can be derived by a transformation into a rotating coordinate system, a concept used, e.g., in NMR to solve the Bloch equations. Following the notations of standard textbooks¹³ we will calculate both the exact solution and the so-called adiabatic approximation.

For the above field configuration the Pauli equation reads

$$i\hbar \frac{\partial}{\partial t} |\Psi(t)\rangle = H(t) |\Psi(t)\rangle = -\mu B \begin{bmatrix} 0 & e^{-i\omega t} \\ e^{i\omega t} & 0 \end{bmatrix} |\Psi(t)\rangle \quad (1)$$

with the eigenvalues $E_{1,2} = \pm \mu B = \hbar\omega_L/2$ (ω_L is the Larmor frequency). Initially (i.e., at $t=0$) the associated eigenvectors $|n(t)\rangle$ ($n=1,2$) are oriented along the $\pm \hat{x}$ direction.

The Hamiltonian $H(t)$ can be diagonalized by the unitary transformation $|\Psi(t)\rangle = U(t) |\Phi(t)\rangle$, with $U(t) = \exp(-i\omega t\sigma_z/2)$, which is equivalent to the transformation into a reference frame rotating with angular frequency ω around the \hat{z} axis. The matrix $U(t)$ also describes the time evolution of the eigenvectors $|n(t)\rangle = U(t) |n(0)\rangle$. In the rotating frame the Pauli equation takes the form

$$i\hbar \frac{\partial}{\partial t} |\Phi(t)\rangle = \left[U^\dagger(t) H(t) U(t) - i\hbar U^\dagger(t) \frac{\partial}{\partial t} U(t) \right] |\Phi(t)\rangle = \frac{1}{2} (\hbar\omega_L \sigma_x - \hbar\omega \sigma_z) |\Phi(t)\rangle. \quad (2)$$

Since the eigenvectors are collinear with the \hat{x} direction, the diagonal term of Eq. (2) is that one which is proportional to σ_x whereas the other—proportional to σ_z —is nondiagonal. Therefore, with the usual notation $\dot{U} = \partial U/\partial t$, the relation $\langle n(0) | U^\dagger(t) \dot{U}(t) | n(0) \rangle = 0$ holds, which is essential for the adiabatic theorem and which also satisfies the parallel transport law.¹⁴ To obtain the adiabatic approximation, the second term of Eq. (2) is neglected for $\omega_L \gg \omega$, leading immediately to

$$|\Psi(\tau)\rangle_{\text{ad}} = U(\tau) \exp(-i\omega_L \tau \sigma_x/2) |\Psi(0)\rangle. \quad (3)$$

The exact solution of Eq. (3) is

$$|\Psi(\tau)\rangle = U(\tau)\exp[-(i/2)\boldsymbol{\alpha}(\tau)\cdot\boldsymbol{\alpha}]|\Psi(0)\rangle, \tag{4a}$$

with $\boldsymbol{\alpha}(\tau) = (\omega_L, 0, -\omega)\tau$. However, this solution has to be generalized still further,

$$|\Psi(\tau, t_0)\rangle = U(\tau)\exp(-(i/2)[\omega_L\tau\{\sigma_x \cos(\omega t_0) + \sigma_y \sin(\omega t_0)\} - \omega\tau\sigma_z])|\Psi(0)\rangle, \tag{4b}$$

by taking into account that the axis of rotation

$$\hat{\boldsymbol{a}}(t_0) = (\omega_L \cos(\omega t_0), \omega_L \sin(\omega t_0), -\omega)/(\omega_L^2 + \omega^2)^{1/2} \tag{5}$$

depends on the specific moment of time t_0 each neutron enters the rotating-field region.

In Eq. (4b) the phase $\delta = \omega_L\tau$ is the so-called *dynamical* phase. It depends on both the strength of the magnetic field and the interaction time. Whereas, it is the matrix

$$U(\tau) = \exp(-i\omega\tau\sigma_z/2) = \exp(-i\gamma\sigma_z/2)$$

which characterizes the *purely geometrical* change of the system, namely, the solid angle $\gamma = \omega\tau$ subtended by the varying field direction, and which consequently causes the geometric phase shift $\Gamma = -\gamma$.^{10,15}

The polarization of a neutron beam is defined as the expectation value of the Pauli spin operator, $\mathbf{P} = \langle\Psi|\boldsymbol{\sigma}|\Psi\rangle/\langle\Psi|\Psi\rangle$. However, it can be interpreted also as an interference phenomenon of two orthogonal states. Any change of the neutron polarization reflects phase differences between these states and can be used therefore to observe additional geometric effects on the phase.^{5,16}

Figure 1 shows a schematic sketch of the experimental setup at the 250-kW TRIGA reactor, Vienna. A pair of Heusler crystals is used to monochromatize ($\lambda = 1.5 \text{ \AA}$) and to polarize the incident neutron beam ($|\mathbf{P}_i| \approx 0.95$) as well as to analyze its final polarization state \mathbf{P}_f . Adiabatic spin turn devices allow us to set and independently

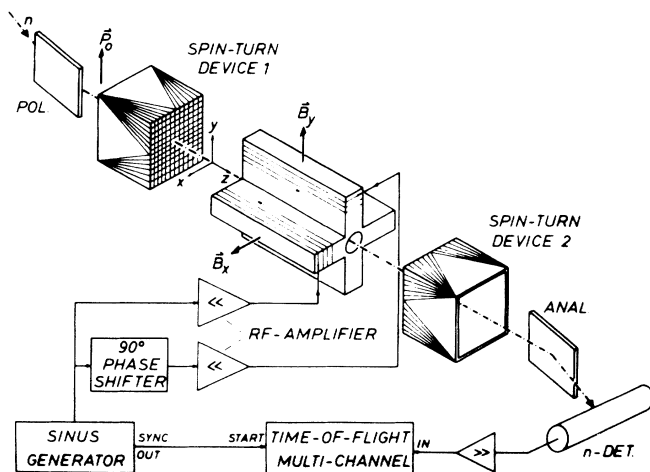


FIG. 1. Sketch of the experimental setup.

analyze the beam polarization consecutively along all three orthogonal directions of space and hence to determine all elements of the (3×3) matrix \underline{P} which describes the change of the polarization vector along the neutron trajectory between polarizer and analyzer, i.e., $\mathbf{P}_f = \underline{P}\mathbf{P}_i$.

The rotating magnetic field is produced by two mutually orthogonal split pair coils of $l = 10$ cm length along the beam path which are driven with a relative phase shift of 90° . At a frequency of $\nu = 26373$ Hz the field rotates just by an angle of 2π during the transmission time $\tau = 37.9 \mu\text{s}$ of the neutrons through the coils. A field amplitude of up to 40 G has to be applied to assure adiabaticity over the whole frequency range $4 \leq \nu \leq 41$ kHz, which corresponds to field rotation angles of $0.3\pi \leq \gamma \leq 3.1\pi$ during the neutron passage.

A time-of-flight multichannel detector triggered periodically by the signal fed to the coils allows us to correlate the time t_0 at which each neutron enters the rotating-field region with the respective field direction. Unless stated otherwise, the presented data are corrected for the unavoidable time-of-flight broadening ($\Delta\lambda/\lambda \approx 1.5\%$) along the 1.2-m distance between the field coils and the detector (effective thickness ≈ 3.5 mm).

To demonstrate the additional, purely geometric, phase effect we analyze the change of the polarization vector along the \hat{y} and the \hat{z} directions. From Eq. (4b) the element P_{yy} of the polarization transfer matrix \underline{P} (i.e., initial and analyzed polarization directions along \hat{y}) follows as

$$P_{yy}(a, \gamma, t_0) = \cos\gamma \cos\frac{2a}{2} + \frac{\gamma}{a} \sin\gamma \sin a - \frac{\delta^2}{a^2} \times \cos(2\omega t_0 + \gamma) \sin\frac{2a}{2} - \frac{\gamma^2}{a^2} \cos\gamma \sin\frac{2a}{2}. \tag{6}$$

Figure 2 shows the measured, uncorrected neutron intensities versus time t_0 for constant frequency $\nu = 14768$ Hz but different amplitudes (i.e., different Larmor frequencies ω_L and different total phase angles a) of the rotating field. They are related to the matrix element P_{yy} via $I = (1 + DP_{yy})I_s$, where the shim intensity for complete depolarization (I_s) and the residual depolarization (D) of the empty apparatus can be measured separately. A least-squares fit of the data according to Eq. (6) yields a geometric phase shift $\gamma = 1.12\pi$, in full agreement with the expected value. Figure 3 shows the measured intensity profiles on a reduced time scale for a series of different frequencies but with constant amplitude $B = 38$

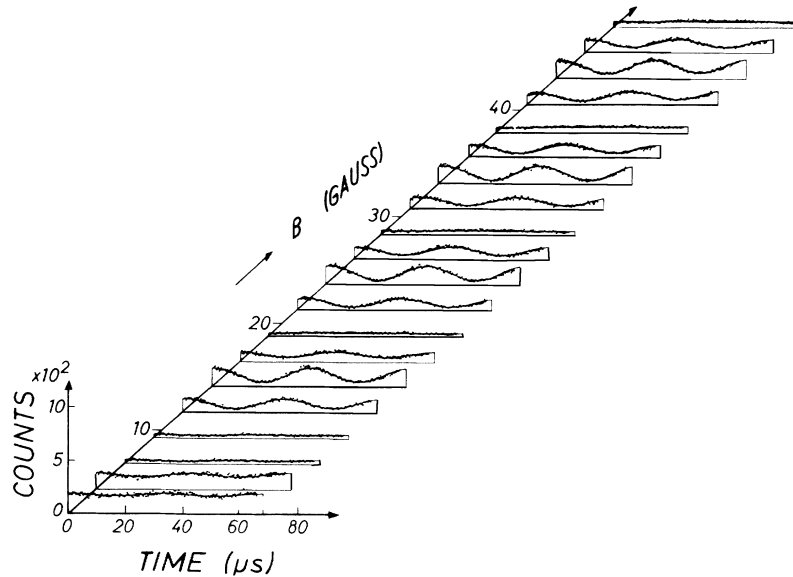


FIG. 2. Time-resolved neutron intensity for different amplitudes of the magnetic field rotating with a frequency $\nu=14768$ Hz. Both the incident polarization and the analyzer were aligned parallel to the \hat{y} direction thus yielding the element P_{yy} of the polarization transfer matrix \underline{P} (see text).

G, corresponding to a Larmor frequency $\omega_L = 698$ kHz. The adiabaticity condition $\omega_L \gg \omega$ is well fulfilled in this case and the total phase angle $\alpha = \tau(\omega_L^2 + \omega^2)^{1/2} \approx \omega_L \tau$ is nearly independent of ω . Hence the observed behavior is characterized by the third term of Eq. (6) and the phase shift of the intensity pattern with increasing frequency, which is indicated by the dot-dashed line, is a direct measure of the geometric phase shift $\Gamma = -\gamma$.

Three of these frequencies deserve special attention, namely, 4266, 22040, and 30606 Hz, which correspond to field rotation angles of 0.323π , 1.67π , and 2.32π . They all have approximately the same relative offset $\pm 0.3\pi$ from either zero rotation angle or the full 2π cycle. However, the sign has no influence since P_{yy} depends quadratically on the rotation frequency and the final Hamiltonian $H(\tau)$ is the same for all three frequencies. For constant field amplitude the dynamical phase $\delta = \omega_L \tau$ is identical for all these cases. Therefore it is only the geometric property, namely, the angle γ

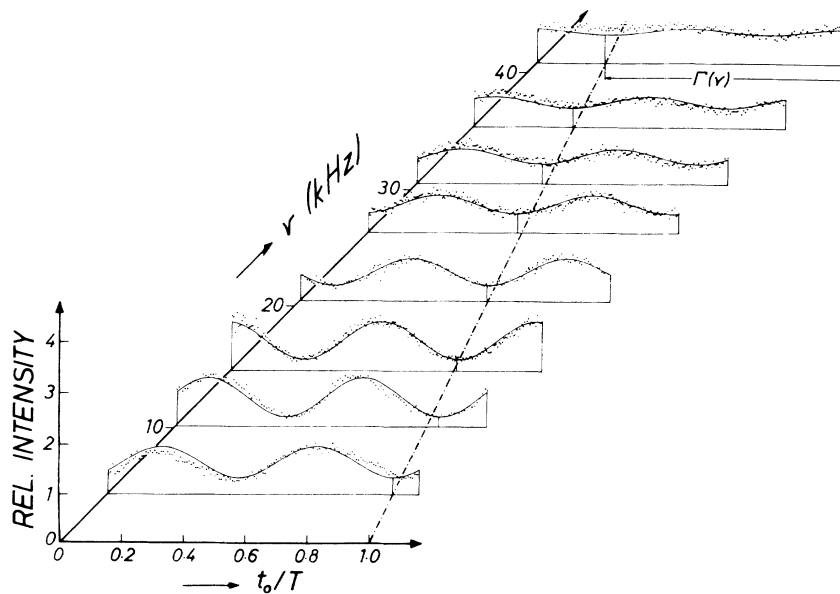


FIG. 3. P_{yy} intensity vs reduced time t_0/T ($T = \nu^{-1}$) for different rotation frequencies at constant field amplitude $B = 38$ G. The dot-dashed line indicates the linear increase of the geometric phase shift $\Gamma(\nu)$ with increasing frequency.

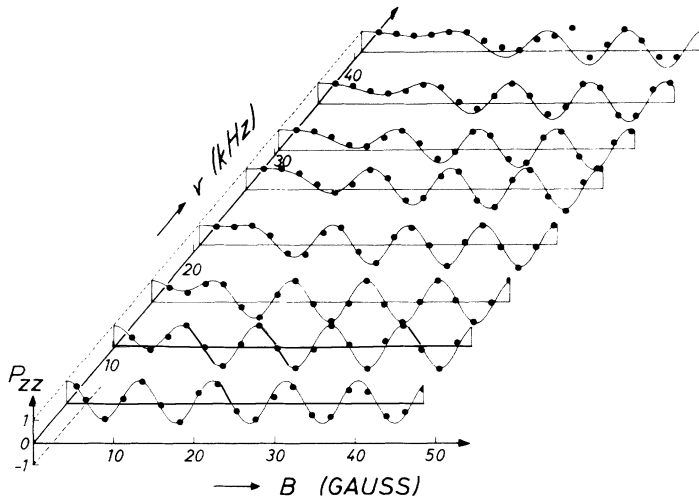


FIG. 4. Polarization change along the \hat{z} direction as a function of the applied field amplitude for different rotation frequencies. It can be seen that the amplitude has to be about 40 G to ensure adiabaticity in the whole frequency range.

subtended by the rotating magnetic field, which differs and consequently causes the unequal phase shifts. Notice that $\gamma_{4266} = 0.323\pi$ and $\gamma_{30606} = 2.32\pi$ differ by approximately 2π and hence can be distinguished here only by tracing the phase shift via intermediate frequencies.

The polarization change along the \hat{z} direction,

$$P_{zz}(\alpha) = \cos \frac{2\alpha}{2} + \frac{1}{\alpha^2} (\gamma^2 - \delta^2) \sin \frac{2\alpha}{2}, \quad (7)$$

is solely determined by the angle α . In the adiabatic limit α becomes equal to the dynamical phase δ and hence no geometric effect should be observable. This behavior is verified in Fig. 4 which shows the element P_{zz} of the polarization transfer matrix \underline{P} as a function of the field amplitude for different frequencies. But due to the dependence of α on γ ($\alpha^2 = \delta^2 + \gamma^2$) the geometric phase influences the polarization not only in the adiabatic but also in the nonadiabatic regime and thus enables one to differentiate easily between the above-mentioned frequencies. In fact, this corresponds to a utilization of nonadiabatic effects caused by the nondiagonal term $U^\dagger(t)\dot{U}(t)$ of Eq. (2), which also reflects the purely geometric evolution of the system.

To summarize, we note that the use of time-dependent rotating magnetic fields allowed us—in extension and continuation of the first measurements of Berry's topological phase with polarized neutrons by Bitter and Dubbers⁵—to reveal geometric phase effects also for noncyclic evolutions. Varying the direction as well as the

frequency of the rotation, but keeping the field amplitude constant, it was possible to reach the same final state in parameter space via different paths. The observed phase changes then solely reflected the geometrical evolution of the system although the final state was different from the initial one. It became evident that nonadiabatic effects also depend merely on the geometric nature of the change of parameters, a fact which was used to determine geometric phase differences of 2π without ambiguity.

We thank Professor H. Grosse and Professor A. Zeilinger for critical readings of the manuscript and the Austrian Fonds zur Förderung der Wissenschaftlichen Forschung for financial support (Project No. S42/08).

¹M. V. Berry, Proc. Roy. Soc. London A **392**, 451 (1984).

²F. Wilczek and A. Zee, Phys. Rev. Lett. **52**, 2111 (1984); J. Moody, A. Shapere, and F. Wilczek, Phys. Rev. Lett. **56**, 893 (1986); E. Gozzi and W. Thacker, Phys. Rev. D **35**, 398 (1987).

³J. H. Hannay, J. Phys. A **18**, 221 (1985); M. V. Berry and J. H. Hannay, J. Phys. A **21**, L325 (1988); A. Bhattacharjee and T. Sen, Phys. Rev. A **38**, 4389 (1988).

⁴A. Tomita and R. Y. Chiao, Phys. Rev. Lett. **57**, 937 (1986).

⁵T. Bitter and D. Dubbers, Phys. Rev. Lett. **59**, 251 (1987); D. J. Richardson, A. I. Kilvington, K. Green, and S. K. Lamoreaux, Phys. Rev. Lett. **61**, 2030 (1988).

⁶R. Tycko, Phys. Rev. Lett. **58**, 2281 (1987); D. Suter, K. T. Mueller, and A. Pines, Phys. Rev. Lett. **60**, 1218 (1988).

⁷R. Bhandari and J. Samuel, Phys. Rev. Lett. **60**, 1211 (1988); R. Y. Chiao, A. Antaramian, K. M. Ganga, H. Jiao, and S. R. Wilkinson, Phys. Rev. Lett. **60**, 1214 (1988); R. Simon, H. J. Kimble, and E. G. C. Sudarshan, Phys. Rev. Lett. **61**, 19 (1988); H. Jiao, S. Wilkinson, R. Y. Chiao, and H. Nathel, Phys. Rev. A **39**, 3475 (1989).

⁸D. M. Bird and A. R. Preston, Phys. Rev. Lett. **61**, 2863 (1988).

⁹Y. Aharonov and J. Anandan, Phys. Rev. Lett. **58**, 1593 (1987); M. V. Berry, Proc. Roy. Soc. London A **414**, 31 (1987).

¹⁰T. F. Jordan, Phys. Rev. A **38**, 1590 (1988).

¹¹J. Samuel and R. Bhandari, Phys. Rev. Lett. **60**, 2339 (1988).

¹²Y. S. Wu and H. Z. Li, Phys. Rev. B **38**, 11907 (1988).

¹³A. Messiah, *Quantum Mechanics* (North-Holland, Amsterdam, 1981), Vol. 2.

¹⁴B. Simon, Phys. Rev. Lett. **51**, 2167 (1983).

¹⁵J. Anandan and L. Stodolsky, Phys. Rev. D **35**, 2597 (1987).

¹⁶F. Mezei, in *Imaging Processes and Coherence in Physics*, edited by M. Schlenker *et al.*, Lecture Notes in Physics Vol. 112 (Springer-Verlag, Berlin, 1980), p. 282.